ACS APPLIED MATERIALS & INTERFACES

Research Article

www.acsami.org

Induced Transition of CdSe Nanoparticle Superstructures by Controlling the Internal Flow of Colloidal Solution

Min Su Kim,[†,§] Seulah Lee,[†,§] Ja Hoon Koo,[†] Juree Hong,[†] Yongwon Chung,[†] Kyung Jin Son,[‡] Won-Gun Koh,[‡] and Taeyoon Lee*[,†]

[†]Nanobio Device Laboratory, School of Electrical and Electronic Engineering, and [‡]Biomaterials Laboratory, Department of Chemical and Biomolecular Engineering, Yonsei University, 50 Yonsei-ro, Seodaemun-Gu, Seoul 120-749, Republic of Korea

Supporting Information

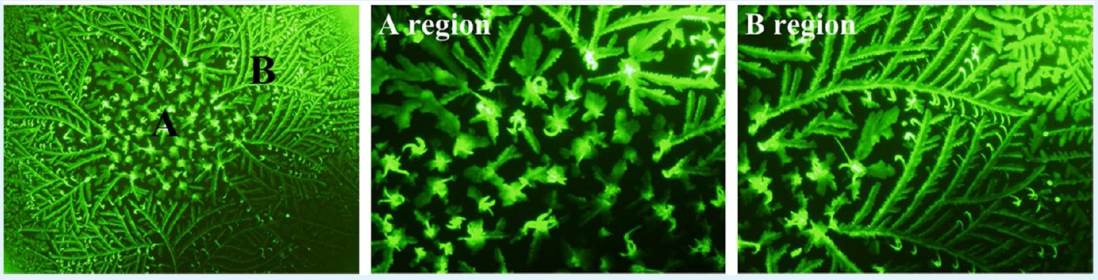

ABSTRACT: The self-assembly behaviors of flow-enhanced CdSe nanoparticle (NP) colloidal systems were investigated, which were systemically prepared by adding ethylene glycol (EG) or acetic acid (AA) to NP suspensions with deionized water (DI water) base. The additive solvents, which had higher boiling points and lower surface tensions than those of the DI water, modified the internal flow of the NP colloidal system, consequently affecting the morphologies of the generated NP superstructures after the full evaporation of their droplets. In flow-enhanced systems, NPs were formed into highly elongated dendrites that stretched from the center region to the edges along the direction of convective flow inside the droplet, while NPs in random drift system were easily aggregated to form cluster-shaped thick dendritic structures. When the volume fraction of EG was increased, the dominant superstructures were changed from dendrites to clusters, which can be mainly attributed to the changes in the dielectric properties of the NP droplets as evaporation proceeded because of the large discrepancy in the vapor pressures of EG and DI water. The balance between the interparticle potentials of electrostatic repulsion and van der Waals attraction was continuously altered, resulting in the formation of clusters with increasing EG ratio. Contrastively, the transition of superstructures could not be observed in the case of colloidal system prepared by mixing DI water and AA, which can be ascribed to the similar vapor pressures of the two solvents; the dielectric properties of the solution mixture was barely changed throughout the steady evaporation process, which resulted in the formation of uniformly distributed highly elongated dendrites. Polarization-dependent imaging experiments and photoluminescence measurements revealed that the stretched dendrites formed under the flow-enhanced conditions showed higher crystallinity than that of the clusters.

KEYWORDS: *CdSe nanoparticle, self-assembly, internal flow, superstructure, Marangoni flow*

1. INTRODUCTION

Superstructures of semiconductor nanoparticles (NPs) are of great interest because of the large variation in their fundamental properties including optical, electrical, magnetic, and catalytic characteristics that can be achieved by varying their sizes and shapes.[1−7] It has also become important to be able to organize the NPs into desired high-dimensional NP superstructures for use in next-generation devices. Among the many kinds of high dimensional NP superstructures, dendritic structure is one of the most interesting because semiconductor NP dendrites have superior artificial light emission and light harvesting properties because of their broad adsorption bands and high Forester resonance energy transfer efficiency.[8,9] However, direct manual handling of NPs to manipulate their overall superstructure is impractical; rather, a solvent-induced self-assembly method can be regarded as a promising bottom-up approach with significant advantages in terms of its cost and simplicity.

There are many challenges associated with building the desired superstructures using solvent-induced self-assembly, since the movement of NPs in a colloidal system is strongly dependent on various interactions such as hydrogen bonding, van der Waals forces, electrostatic forces, dipole interaction, and charge−dipole interaction. These interactions are highly sensitive to the conditions of the colloidal suspensions such as temperature, vapor pressure, and the pH of the solvent. Much effort has been dedicated toward controllably manipulating the colloidal NPs into forming the desired superstructure.[6−12] For

Received: June 13, 2012
Accepted: September 12, 2012
Published: September 12, 2012

example, Sukhanova et al. varied the evaporation temperature to control the morphology of the self-assembled superstructures,[9] Zhang et al. added different concentrations of salt to colloidal suspensions to change the electrostatic interactions between the NPs,[11] and Li et al. tuned the self-assembly of CdTe/polymers using pH stimuli.[12] Most of these previous self-assembly studies focused on controlling the interactions between the NPs in colloidal suspensions. In contrast, few studies have examined on the methods to alter the internal flow of a colloidal solution, which may strongly affect the formation of NP superstructures.

Here, we investigated the effects of controlling the internal flow of colloidal suspensions on the formation of CdSe NP superstructures. To reduce the randomness of the drifting NPs and to enhance the internal flow of the evaporating droplets, we added solvents with lower surface energies and higher boiling points than those of the deionized (DI) water into CdSe NPs-DI water solutions. Specifically, two different NP colloidal systems were prepared: ethylene glycol (EG) and acetic acid (AA) were separately added to NP suspension with DI water base. It could be clearly observed from the fluorescent microscope images that the developed NP superstructures were highly influenced by varying the volume ratios of EG/DI water (V_{eg}/V_{dw}) and AA/DI water (V_{aa}/V_{dw}). Whereas the morphologies of the obtained NP superstructures were changed from dendrites to clusters during evaporation of a NP colloid droplet with high V_{eg}/V_{dw} ratio, only dendritic NP superstructures could be obtained using AA as the additive solvent to induce internal flow of the NP colloid. Photolumisnecence (PL) measurements and polarized micrographs were examined to verify the crystallinity of the obtained superstructures, revealing that dendritic superstructures obtained from the flow-enhanced system exhibit higher crystallniity than those of the clustered superstructures.

2. EXPERIMENTAL SECTION

Glass substrates (2.5 cm^2) were successively cleaned in acetone, isopropyl alcohol, and DI water, followed by nitrogen blowing to dry the substrates. 6-nm-diameter CdSe/ZnS quantum dots (QD) with trioctylephosphine (TOP) ligands in the hydrophobic liquid were purchased from Nanosquare (see Figure S1 in the Supporting Information). This QD solution with 1.0 mg/mL of hydrophilic cysteine hydrochloride (LCys) ligand was sonicated for 1 h to obtain water-solubilized QDs. To enhance the internal flow of the QD-DI water solution, we added EG to 1.0 mg/mL of QD-DI water solution while maintaining the total volume of solvent at 175 μL. To investigate the effect of vapor pressure and dielectric properties of the additive solvent on the resulting superstructures, we prepared a separate NP suspension by adding AA to 1.0 mg/mL of QD-DI water solution while maintaining the total volume of solvent at 175 μL. V_{eg}/V_{dw} ratio and V_{aa}/V_{dw} ratios were varied from 0.16 to 0.5 to investigate the effect of the internal flow in QD-DI water solutions on the resulting superstructures. These mixtures were sonicated for 10 min to obtain well-dispersed QDs in solvent mixtures, and then drop-cast on the cleaned glass substrates. The volume of the droplets was maintained at approximately 5 μL. The droplets were fully evaporated under ambient conditions at room temperature.

The morphologies of the formed superstructures were characterized using a fluorescence microscopy (Olympus IX71) and an atomic force microscopy (AFM, XE-100, Park System). The crystallinity of the organized superstructures was analyzed with a polarizing microscope (Eclipse LV100POL, Nikon). PL spectra in the wavelength range from 300 to 650 nm were obtained using a wide bandgap PL measurement system (Mini PL 5.0, Dongwoo Optron) equipped with a 325 nm He−Cd laser.

3. RESULTS AND DISCUSSION

Panels a and b in Figure 1 show the representative fluorescent micrographs of the dendritic superstructures obtained after the full evaporation of random drift NP droplets and flow-enhanced NP droplets, respectively. The solvent-induced self-assembly of superstructures is highly dependent on the diffusion rate of the suspended colloids in solution during the evaporation of droplets. Thus, EG was added as a minor solvent (in terms of volume) with a higher boiling point and a lower surface tension than the major solvent to generate Marangoni flow, a circulative inward flow that opposes the outward convective flow that acts to replenish the evaporation at the edge of the droplet.[13] As shown in Figure 1a, the dendritic superstructures grown using the random drift NP colloids (60 μg QD + 175 μL DI water) seemed to have several randomly scattered botanical roots from which the branches were stretched out in a radial direction. Typically, the branches were stretched out symmetrically for up to three-four generations with short lengths. The lateral dimension of the dendrites was observed to be gradually decreasing from the center toward the edge region. The individual branches of the superstructures seemed to be considerably thick and wide, based on the color contrast in the micrographs. Closer examination of the fluorescent micrographs revealed that the length of the branches varied from 40 to 400 μm, and their widths decreased prominently from approximately 30 to 1−2 μm toward the end of the branches, which had sharp ends. In contrast, the dendrites that formed in the flow-enhanced NP colloid system (V_{eg}/V_{dw} of 0.16) shown in Figure 1b had highly stretched branches with a fairly uniform interbranch distance of approximately 20 μm. The branches extended out as far as 500 μm. The width of the first generation branches was about 12

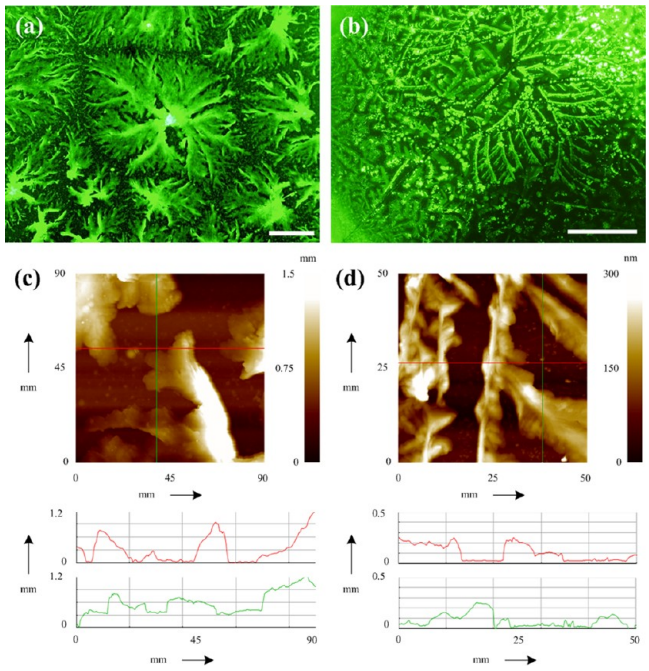

Figure 1. (a, b) Fluorescent micrographs and (c, d) atomic force microscopy images of the CdSe NP superstructures generated by evaporation of (a) DI water only and (b) a solvent with a V_{eg}/V_{dw} ratio of 0.16. The concentration of QDs in the solvent was fixed at 0.33 mg/mL and the evaporation of the droplets was conducted under air ambient at room temperature. Scale bars in a and b represent 200 μm.

dx.doi.org/10.1021/am301798r | ACS Appl. Mater. Interfaces 2012, 4, 5162−5168

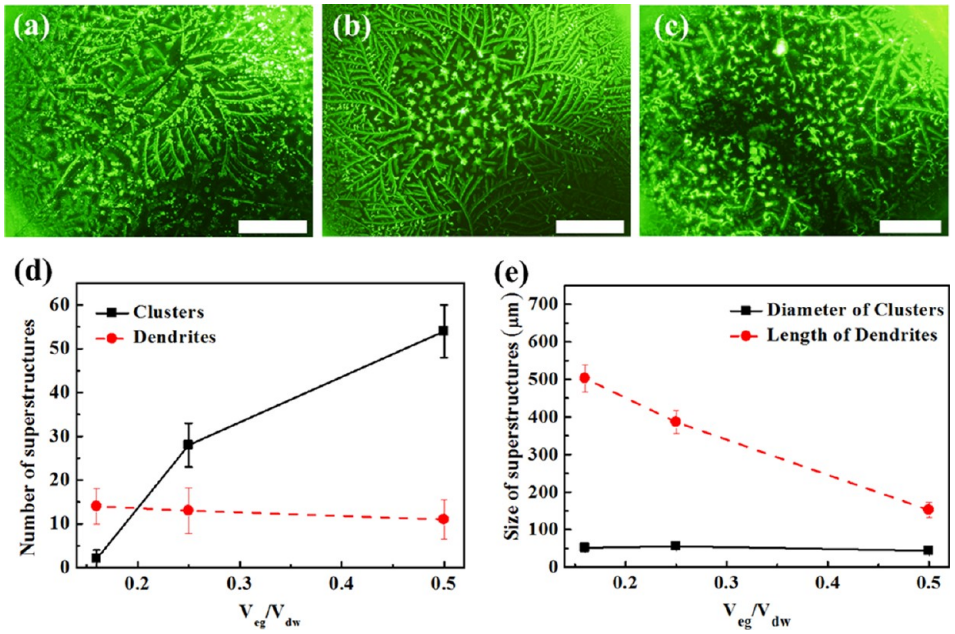

Figure 2. Fluorescent micrographs of CdSe NP superstructures developed after the full evaporation of solutions with a V_{eg}/V_{dw} ratio of (a) 0.16, (b) 0.25, and (c) 0.5. The concentration of NPs in all solutions was fixed at 0.33 mg/mL and all droplets were evaporated under ambient conditions at room temperature. (d) Population of superstructures and (e) Physical dimensions produced from various V_{eg}/V_{dw} solutions. Scale bars in (a–c) indicate 200 μm.

μm and remained this wide until the ends of the branches, while the width of the branches narrowed slightly to 11, 10, and 8 μm as the generations proceeded. Figure 1c, d exhibit the typical AFM images obtained from the samples shown in Figure 1a, b, respectively. The mean thickness of the dendritic superstructures formed by the random drifting colloids was approximately 1 μm, whereas that of the dendrites generated from the flow-enhanced colloids was about 240 nm. Superstructures similar to those of symmetric dendrites grown in random drifting NP colloids (Figure 1a) have been found in many other material systems such as CdTe, iron oxide, gold, and copper systems, and the underlying physics of their formation have been studied extensively.[8−12,14−16] However, interpretation of the regularity and crystallinity in superstructures obtained using the flow-enhanced NP solution is at no time easy.

The main parameters of NP superstructure formation, which are related to the internal flow of the droplet, are the evaporation rate (r_{ev}) of the droplet and the diffusion rate (r_{diff}) of the suspended colloids in solution. The latter can be classified further into the translational diffusion rate (r_t) and the orientational diffusion rate (r_{or}). Because NPs cannot organize themselves without a solvent, the morphology of the NP structure is strongly dependent on r_{ev}, which is associated with the freezing rate of the NPs inside the solution.[9] Meanwhile, the factors r_t and r_{or} are related to the mobility of the NPs in solution and the ordering of NPs with identical orientation during the evaporation process, respectively. It has been reported in a previous work of Sukhanova et al. that when a droplet from a colloidal solution with a low r_{ev} and a high r_{or} or r_t is evaporated, highly ordered superstructures with superior crystallinity were obtained.[9] Similarly, adding EG to the NP colloidal dispersion lowered the r_{ev} value of the NP solution, because of the lower vapor pressure of EG (0.06 mmHg)[17] compared to that of the DI water (17.3 mmHg).[18] In addition, it also leads to increasing the value of r_t because of the generation of Marangoni flow. As a result, the dominant superstructures that formed changed from thick, irregularly shaped dendritic structures (Figure 1a) to more uniformly shaped dendrites with higher dimensions (Figure 1b).

To investigate the effect of varying the volume fraction of EG on the growth of the superstructures, the V_{eg}/V_{dw} ratio of the NP solutions was varied and these solutions were separately drop-cast to examine the resulting morphologies of the superstructures after full evaporation. Figure 2a–c are the representative fluorescent micrographs of the NP superstructures obtained using flow-enhanced solutions with increasing the V_{eg}/V_{dw} ratios from 0.16 to 0.5. When V_{eg}/V_{dw} was 0.16 (Figure 2a), the dominant superstructures obtained were dendrites, and superstructures with other shapes were rarely observed. As the V_{eg}/V_{dw} ratio increased, there was a clear transition of the dominant superstructures from dendrites to clusters, as shown in the micrographs in Figure 2b, c and the qualitative analyses results presented in Figure 2d, e. Figure 2d and e show qualitative data obtained for the dominant superstructures as the internal flow of the NP droplets was varied. The number of dendrites decreased slightly from 14 to 11 as the V_{eg}/V_{dw} ratio increased, whereas the population of clusters increased drastically from 2 to 54 (Figure 2d). The diameters of clusters remained almost the same at 50 μm, whereas the lengths of dendrites became considerably shorter (502 to 152 μm) as the V_{eg}/V_{dw} ratio increased (Figure 2e).

When the V_{eg}/V_{dw} ratio was increased to 0.25 (Figure 2b), a distinct branch directionality from the near-center region to the edge in a fan-shape was observed. At the center region, which had a radius of approximately 180 μm, short-branched clusters were predominantly found. When the V_{eg}/V_{dw} ratio was increased further to 0.5 (Figure 2c), the dominant superstructures formed were clusters. A few dendrites with very short branches were also observed, but there was no directionality to the branches. These results indicate that the volume fraction of EG in the NP colloidal solution has an influence on the internal

flow; however, the formation of short-branched clusters by increasing the volume fraction of EG cannot be intuitively comprehended. We believe that the observed transition in NP superstructures was caused mainly by the considerably large discrepancy in the vapor pressures of DI water and EG. For example, when the QD solutions were dropped on the glass substrates, the contact line that formed between the droplet and the glass substrate was pinned and then evaporation started (see Figure 2b). Regularly shaped dendrites with branches in a fan-shape starting from the edge of the droplet toward the center were formed due to the induced Marangoni flow and the accompanying convective flow. However, as evaporation proceeded, the contact line receded toward the center region. At this point, r_{diff} and r_{ev}, both of which are directly associated with the higher viscosity of the NP droplet, dropped substantially owing to the faster evaporation rate of DI water than EG. When EG became the dominant solvent in the droplet, the diffusion of NPs inside the droplet can be assumed as follows

$$D = K_B T/(6\pi\eta r_a) \quad (1)$$

where D is the diffusion coefficient of a spherical Brownian particle, $K_B T$ is the thermal energy, η is the viscosity of the solvent suspending the particle, and r_a is the particle's hydrodynamic radius.[19] Because the viscosity of EG (1.61×10^{-2} Ns/m^2)[20] is considerably higher than that of DI water (8.94×10^{-4} Ns/m^2),[21] the r_{diff} of the suspended colloids would have decreased continuously as the V_{eg}/V_{dw} ratio increased over time, and consequently the NPs would not have been free to move to become more highly ordered. The leftover NPs would therefore have been prone to form clusters (the detailed reason for this will be discussed later in the description of Figure 3). This explains the transition in the

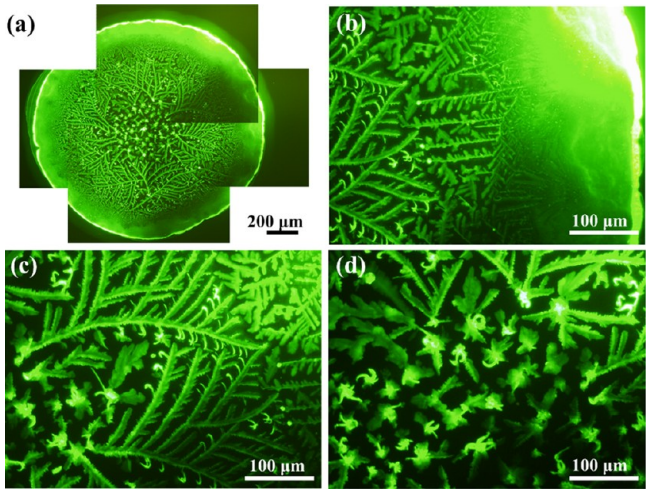

Figure 3. Fluorescent microscope images of the CdSe NP superstructures produced after the full evaporation of a droplet with V_{eg}/V_{dw} ratio of a 0.25: (a) stitched-together image of the whole region, (b) edge, (c) inner region, and (d) center of the droplet.

superstructures obtained from dendrites to clusters toward the center of the droplet, and also explains why the area covered by clusters at the center of the NP droplets was increased in Figure 2c, where a higher volume fraction of EG was used.

A stitched image of entire superstructures produced in solution with a V_{eg}/V_{dw} ratio of 0.25 is represented in Figure 3a) to closely examine the variable shapes of the NP superstructures according to the position after the evaporation of a flow-enhanced NP droplet. The produced superstructures exhibited different shapes according to their position of formation as follows: a relatively thick coffee ring of ~200 μm was observed at the edge of the droplet (Figure 3b), whereas at the inner region, long dendrites with three-four generations were diverged from the coffee ring and stretched out toward the center of the droplet, until they were approximately 180 μm away from the center (Figure 3c). The center region with a radius of ~180 μm was covered with clusters (Figure 3d). Although the transition of superstructures according to location could be explained by the internal flow of the droplet and the changes in the r_{diff} and r_{ev} values with respect to the V_{eg}/V_{dw} ratio, it is unclear why superstructures with specific morphologies (either clusters or dendrites) formed. Zhang et al. reported that the stability of NP colloidal suspensions is strongly associated with the final morphologies of the generated superstructures.[11] The colloidal stability of the NPs in solvent can be characterized by the Derjaguin–Landau–Verwey–Overbeek (DLVO) theory, which states that the stability of NPs in solution is closely related to their electrostatic potential (Ψ_{elec}), van der Waals potential (Ψ_{vdW}), dipolar interaction potential (Ψ_{dipole}), and charge-dipole interaction potential ($\Psi_{charge\text{-}dipole}$).[11,22−25] Here, Ψ_{elec} between charged particles of the same polarity results in repulsion, whereas the other three potentials (Ψ_{vdW}, Ψ_{dipole}, and $\Psi_{charge\text{-}dipole}$) generate attractive forces between particles. Since the QDs used in this experiment were uniformly capped with L-Cys ligands, Ψ_{dipole} and $\Psi_{charge\text{-}dipole}$, which originate from surface defects and nonuniform ligand capping, could be considered small enough to be neglected. Thus, we could simplify that the balance between Ψ_{elec} and Ψ_{vdW} mainly determines the stability of the colloidal dispersion and the transition in the morphologies of the resulting superstructures. These two potential values can be calculated as follows

$$\Psi_{elec}(r) = 2\pi\varepsilon_s\varepsilon_0\alpha\Psi_0^2\ln[1 + \exp(-\alpha\kappa(R - 2))] \quad (2)$$

$$\Psi_{vdW}(r) = \frac{A_H}{6}\left[\frac{2}{R^2 - 4} + \frac{2}{R^2} + \frac{R^2 - 4}{R^2}\right] \quad (3)$$

where r is the distance between particles, ε_s is the relative dielectric constant of the solvent, ε_0 is the vacuum dielectric constant, Ψ_0 is the surface potential of NPs, α is the radius of NPs ($R = r/\alpha$), κ is the inverse Debye length, and A_H is the Hamaker constant of NPs (6.216×10^{-20} J for CdSe).

At the onset of droplet deposition on the surface of a glass substrate, the droplet spread to obtain equilibrium wet spreading, due to relaxation of the surface tension.[26] After the contact diameter reached its maximum, it receded back until the contact line was pinned. During this state, NPs in the solution were stable as colloids, because Ψ_{elec} between the NPs was larger than Ψ_{vdW}. This resulted in the deposition of a coffee-ring stain; in other words, the NPs were not transformed into any particular superstructures but rather deposited uniformly. As evaporation proceeded, meaning that the V_{eg}/V_{dw} ratio increased because of the faster evaporation of DI water than EG, Ψ_{elec} decreased continuously because the dielectric constant of EG ($\varepsilon_s = 38.66$)[27] is nearly half that of DI water ($\varepsilon_s = 80.37$)[27] at room temperature. The charged NPs started to aggregate to form superstructures with higher dimensions with decreasing Ψ_{elec}, but there was still a significant amount of repulsive forces, and the NPs grew linearly to repel

each other as far as possible, resulting in the formation of elongated superstructures.[11] With further evaporation, Ψ_{elec} decreased significantly, and the NPs comprising the superstructures did not have enough potential to repel the NPs that attached to the sides of the superstructures, resulting in a smaller angle between the stretched branches. At the final stage of evaporation, the repulsive force between NPs became negligibly small, and the aggregation tendency of the NPs led them to form clusters. This model is in good agreement with the observed transition in superstructures from dendrites to clusters.

A comparative analysis on the resulting NP superstructures was conducted by changing the additive solution from EG to AA, which also has a lower surface energy and higher boiling point than that of DI water, but considerably higher vapor pressure (16.2 mmHg, same order as that of DI water)[21] and lower dielectric constant (ε_s = 6.15)[21] than those of EG. Figure 4a–c shows the representative fluorescent micrographs of the

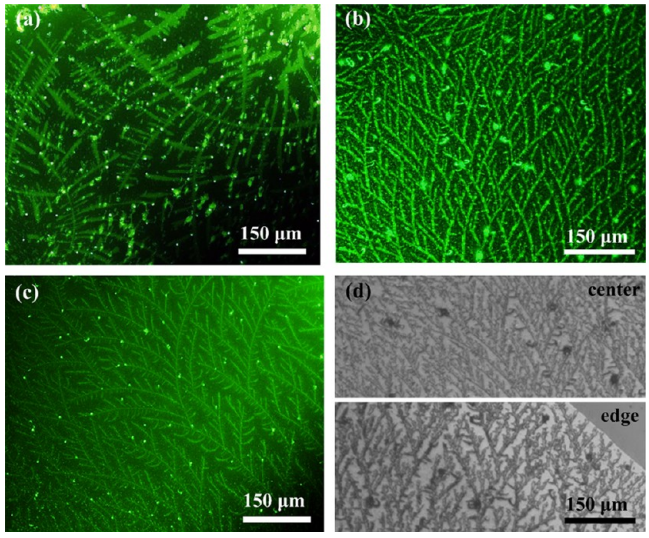

Figure 4. Fluorescent micrographs of CdSe NP superstructures developed after the full evaporation of solutions with a V_{aa}/V_{dw} ratio of (a) 0.16, (b) 0.25, and (c) 0.5. The concentration of NPs in all solutions was fixed at 0.33 mg/mL and all droplets were evaporated under ambient conditions at room temperature. (d) Optical images of NP superstructures formed according to different locations of the droplet with V_{aa}/V_{dw} ratio of 0.25.

NP superstructures obtained using AA-added flow-enhanced solutions with V_{aa}/V_{dw} ratios of 0.16, 0.25, and 0.5, respectively. The obtained dominant superstructures were highly elongated dendritic branches in all three NP colloidal suspensions with different V_{aa}/V_{dw} ratios. Even though the dielectric constant of AA was nearly six times lower than that of EG, AA and EG were added as minor solvents to the NP suspension with DI water base, and hence the total dielectric constant (ε_t) of the two flow-enhanced NP colloidal systems were similar. In specific, ε_t of flow-enhanced NP colloidal system with V_{aa}/V_{dw} ratios 0.16, 0.25, and 0.50 were 74.4, 72.0, and 66.5, respectively, and ε_t of flow-enhanced NP colloidal system with V_{eg}/V_{dw} ratios 0.16, 0.25, and 0.50 were 69.8, 65.5, and 55.6, respectively. Thus, highly elongated dendritic superstructures could also be formed by evaporation of AA-added NP colloidal suspensions.

Figure 4d shows that at the center and edge regions of the evaporated NP colloidal droplet with V_{aa}/V_{dw} ratio of 0.25, the same dendritic superstructures with almost identical lengths and density were formed. The morphological transition of NP superstructures from dendrites to clusters could not be observed according to the location, even when the V_{aa}/V_{dw} ratios were changed from 0.16 to 0.50. The average lengths of the dendrites were shortened with decreasing the V_{aa}/V_{dw} ratio, which is consistent with the results of EG-added flow-enhanced solutions with varying V_{eg}/V_{dw} ratios. It can be attributed to the decreased Ψ_{elec} in the NP colloidal suspensions with higher V_{aa} or V_{eg}, because the dielectric constant of AA and EG are proportionally related to Ψ_{elec}, as described in eq 2. On the basis of these results, it seems that the main source that affected the transition of NP structures from dendrites to clusters was the vapor pressure of the additive solution. When EG was used as the additive solvent, the ratio of V_{eg}/V_{dw} was continuously increased as evaporation proceeded because of the high vapor pressure of DI water. It resulted in the continuous decrease of dielectric constant and corresponding Ψ_{elec} as the evaporation proceeded. Consequently, when Ψ_{elec} was low enough, clusters were formed instead of dendrites due to the aggregation tendency of the NPs. On the other hand, the V_{aa}/V_{dw} ratio could be sustained throughout the evaporation process due to the similar evaporation rates of AA and DI water, and thus the dielectric properties of the AA-added NP colloidal suspension was merely changed during the evaporation. This means that Ψ_{elec} was at the necessarily high level for the NPs to repel each other and form highly elongated dendritic superstructures throughout the entire evaporation process. In addition, relatively low r_{ev} and high r_{diff} resulting from the Marangoni flow could be maintained until the NP droplet was fully evaporated, which resulted in the highly ordered NP superstructures.

Figure 5a illustrates the representative optical transmission image obtained from the center of the superstructures obtained from a NP droplet with a V_{eg}/V_{dw} ratio of 0.25. Figure 5b is the optically polarized micrograph of Figure 5a, and Figure 5c is the crossed polarizing image obtained by rotating the sample stage 52° clockwise from its position in Figure 5b. The polarized optical micrographs were taken since they can be used to determine the crystallinity of the developed superstructures, as evidenced from previous reports;[8,10,11] it was described that when dendrites are ordered in a certain preferential directions, they were referred as dendrite-like polycrystalline structures. The polarization-dependent imaging experiments confirmed that the cluster superstructures had low polarity, as there was no distinct variation in the brightness contrast of the superstructures at different polarizing angles. Figure 5d is the representative optical transmission image of the dendrites grown in the inner region. Figure 5e is the polarized micrograph of Figure 5d, and Figure 5f is the crossed polarizing image obtained when the sample stage was rotated 52° clockwise from Figure 5d. The crystal orientations of individual NPs were highly ordered along the branch of the dendrite, as shown in Figure 5e, f. The dark dendrite at the left bottom corner of Figure 5e corresponds to the bright dendrite in the left side of Figure 5f, and the bright dendrites located at the center of Figure 5e correspond to the dark dendrites in Figure 5f. It can be inferred that the ordering of crystallinity was maintained only in the same dendrite; these results provide a clear demonstration of the birefringence of the formed dendrites.

Figure 6 shows the PL spectra obtained from dendrites in region (A) (square symbols) and clusters in region (B) (circle

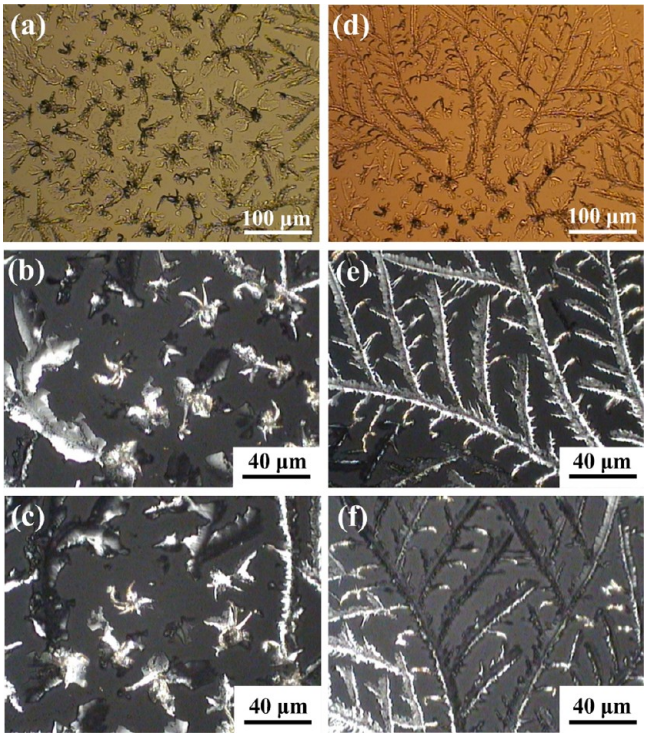

Figure 5. Parallel polarizing images of (a) clusters and (d) dendrites formed using the 0.25 V_{eg}/V_{dw} solution. (b, c, e, f) Crossed polarizing images of (b, c) a and (e, f) d, respectively, where c and f are images taken of samples rotated 52° clockwise from b and e, respectively.

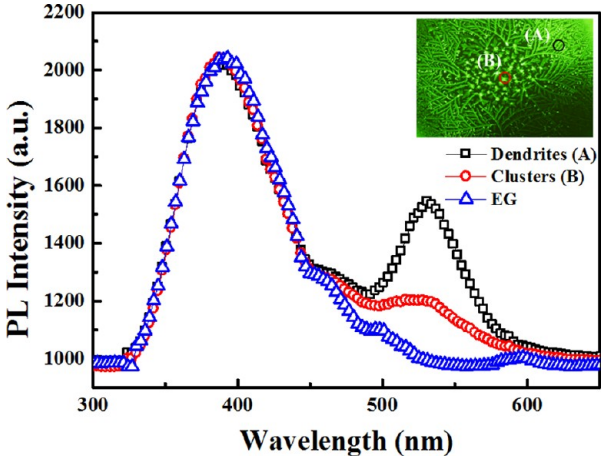

Figure 6. PL spectrum of the CdSe NP superstructures formed using the 0.25 V_{eg}/V_{dw} solution. Inset shows the corresponding measured spots of the clusters and dendrites.

symbols). Two noticeable peaks were observed around 390 and 530 nm. Given the PL spectrum of EG (triangle symbols), the peak around 390 nm presumably originated from the EG solution, while the peak near 530 nm was from the CdSe superstructures. The intensity of the peak near 530 nm obtained from the CdSe dendrites was approximately 2.76 times stronger than that of the CdSe clusters, which indicates the higher crystallinity of the dendritic superstructures than that of the clusters. This result is in good accordance with the results of polarizing microscopy analyses (Figure 5). The full-width-at-half-maximum (fwhm) of the cluster peak was approximately 50.5 nm and that of the dendrite was 42.5 nm. This decrease in the PL line width in parallel with a slight red shift (520 nm for clusters and 532 nm for dendrites) can also be attributed to the higher crystallinity of the dendritic superstructures than that of the clusters, since the process of energy transfer would be more efficient between the NPs constituting the dendrites than the clusters.

4. CONCLUSION

We used CdSe NPs uniformly capped with L-Cys ligands as a model system to investigate the effects of enhancing the internal flow of the NP droplets on the generated superstructures. Mixing two different solvents with dissimilar surface tensions and boiling points induced Marangoni flow inside the NP colloids, thereby affecting the diffusion rate of the NPs. Under the flow-enhanced condition, highly elongated, well-ordered NP dendrites were formed, whereas relatively aggregated thick dendrites were generated under the random drift condition. During evaporation of NP colloids in the EG-added flow-enhanced system, the dielectric constant and viscosity of the NP colloids, and the diffusion rate of the NPs inside the droplet changed because of the substantial difference in vapor pressures of DI water and EG. In conjunction with the DVLO theory, it can be inferred that the balance between the interparticle potentials of electrostatic repulsion and van der Waals attraction changed during evaporation of the NP colloids. This potential change mainly induced the transition in morphology of the superstructures according to the location of the NPs; clusters were formed at the center region and highly elongated dendrites with superior crystallinity were formed at the inner region; these findings were confirmed by polarizing optical and PL analyses. By using AA as the additive solvent, of which the vapor pressure was in the same order as that of DI water, the transition of NP superstructures from dendrites to clusters could be avoided. These results indicate that controlling the formation of self-assembled superstructures with desired morphologies can be feasible by varying the properties of the additive solvent, which can induce Marangoni flow in the NP colloidal system, and we expect that our flow-controlled method can be applicable to many other colloidal systems.

■ ASSOCIATED CONTENT

Ⓢ Supporting Information

Scanning electron microscope image of CdSe/ZnS QDs with trictylephosphine ligands deposited on a silicon substrate by spin-coating. This material is available free of charge via the Internet at http://pubs.acs.org/.

■ AUTHOR INFORMATION

Corresponding Author

*E-mail: taeyoon.lee@yonsei.ac.kr.

Author Contributions

§These authors have equally contributed to this work.

Notes

The authors declare no competing financial interest.

■ ACKNOWLEDGMENTS

This work was supported by the Priority Research Centers Program through the National Research Foundation of Korea (NRF) funded by the Ministry of Education, Science and Technology (2009-0093823). This work was also supported by the KARI-University Partnership program and the Converging

Research Center Program through the Ministry of Education, Science and Technology (2011K000631).

REFERENCES

(1) Alivisatos, A. P. *Science* **1996**, *271*, 933.
(2) Bruchez, M., Jr.; Moronne, M.; Gin, P.; Weiss, S.; Alivisatos, A. P. *Science* **1998**, *281*, 2013.
(3) Zhong, X.; Han, M.; Dong, Z.; White, T. J.; Knoll, W. *J. Am. Chem. Soc.* **2003**, *125*, 8589.
(4) Peng, X.; Manna, L.; Yang, W.; Wickham, J.; Scher, E.; Kadavanich, A.; Alivisatos, A. P. *Nature* **2000**, *404*, 59.
(5) Qian, H.; Dong, C.; Peng, J.; Qiu, X.; Xu, Y.; Ren, J. *J. Phys. Chem. C* **2007**, *111*, 16852.
(6) Zhuang, J.; Wu, H.; Yang, Y.; Cao, Y. C. *Angew. Chem., Int. Ed.* **2008**, *47*, 2208.
(7) Yun, S. H.; Yoo, S. I.; Jung, J. C.; Zin, W. C.; Sohn, B. H. *Chem. Mater.* **2006**, *18*, 5646.
(8) Sukhanova, A.; Baranov, A. V.; Perova, T. S.; Cohen, J. H. M.; Nabiev, I. *Angew. Chem., Int. Ed.* **2006**, *45*, 2048.
(9) Sukhanova, A.; Volkov,Y.; Rogach, A. L.; Baranov, A. V.; Susha, A. S.; Klinov, D. ; Oleinikov, V.; Cohen, J. H. M.; Nabiev, I. *Nanotechnology* **2007**, *18*.
(10) Sun, H.; Wei, H.; Zhang, H.; Ning, Y.; Tang, Y.; Zhai, F.; Yang, B. *Langmuir* **2011**, *27*, 1136.
(11) Zhang, H.; Wang, D. *Angew. Chem., Int. Ed.* **2008**, *47*, 3984.
(12) Li, J.; Liu, B. *Langmuir* **2006**, *22*, 528.
(13) Lim, J. A.; Lee, W. H.; Lee, H. S.; Lee, J. H.; Park, Y. D.; Cho, K. *Adv. Funct. Mater.* **2008**, *18*, 229.
(14) Liu, H.; Zhao, X. *Appl. Phys. Lett.* **2007**, *90*.
(15) Jasuja, K.; Berry, V. *ACS Nano* **2009**, *3*, 2358.
(16) Dong, W.; Li, X.; Shang, L.; Zheng, Y.; Wang, G.; Li, C. *Nanotechnology* **2009**, *20*.
(17) Flick, E. W. *Industrial Solvents Handbook*; William Andrew: Norwich, NY, 1998.
(18) Speight, J. G. *Lange's Handbook of Chemistry*; McGraw-Hill: New York, 2005.
(19) Einstein, A. *Ann. Phys.* **1905**, *322*, 549.
(20) Elert, G. *The Physics Hypertextbook 2007*; http://www.hypertextbook.com/physics.
(21) Weast, R. C.; Astle, M. J.; Beyer, W. H. *CRC Handbook of Chemistry and Physics*; CRC Press: Boca Raton, FL, 1988.
(22) Ducker, W. A.; Senden, T. J.; Pashley, R. M. *Nature* **1991**, *353*, 239.
(23) Wu, W.; Giese, R. F.; Van Oss, C. J. *Colloids Surf., B* **1999**, *14*, 47.
(24) Wu, J.; Zhang, H.; Zhang, J.; Yao, T.; Sun, H.; Yang, B. *Colloids Surf., A* **2009**, *348*, 240.
(25) Dong, J.; Corti, D. S.; Franses, E. I.; Zhao, Y.; Ng, H. T.; Hanson, E. *Langmuir* **2010**, *26*, 6995.
(26) Lim, J. A.; Lee, W. H.; Lee, H. S.; Lee, J. H.; Park, Y. D.; Cho, K. *Adv. Funct. Mater.* **2008**, *18*, 229.
(27) Zahn, M.; Ohki, Y.; Fenneman, D. B.; Gripshover, R. J.; Gehman, V. H., Jr. *Proc. IEEE* **1986**, *74* (9), 1182.